Supporting Information

Extraction of Backscattering and Absorption Coefficients of Magnetite Nanosphere Composites from Light Scattering Measurements: Implications for Optomagnetic Sensing.

Junxin Wang[1], Changgang Xu[1,2,*], Hui Xiong[1,3], Yuanyuan Han[1], Annica M. Nilsson[1,4], Mattias Strömberg[1], Tomas Edvinsson[1], and Gunnar A. Niklasson[1,*]

1. Department of Materials Science and Engineering, The Ångström Laboratory, Uppsala University, PO Box 35, SE-75103 Uppsala, Sweden

2. School of Materials Science and Engineering, Xi'an University of Science and Technology, Xi'an 710054, China

3. School of Mathematics and Physics, Hubei Polytechnic University, Huangshi 435003, Hubei, China

4. Department of Civil and Industrial Engineering, The Ångström Laboratory, Uppsala University, P.O. Box 169, SE-75104 Uppsala, Sweden

Corresponding Authors

*E-mail: (G.A.N.) Gunnar.Niklasson@angstrom.uu.se

*E-mail: (C.G.X.) changgangxu@xust.edu.cn

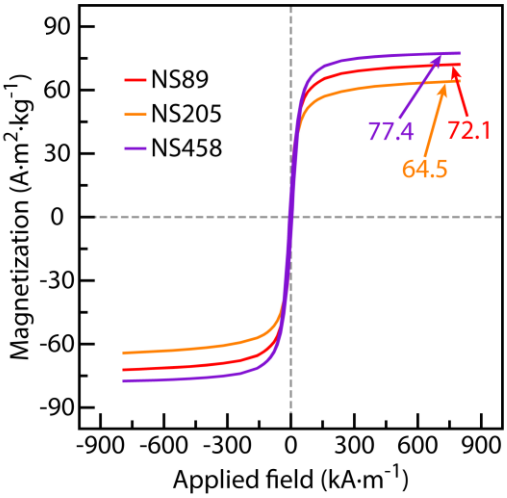

Figure S1. Magnetization curves (M-H) of the Fe_3O_4 nanoparticle samples with average diameters of 89 ± 19 nm (NS89; red), 205 ± 27 nm (NS205; orange) and 458 ± 137 nm (NS458; violet). Complete loops were measured and the samples showed no hysteresis.

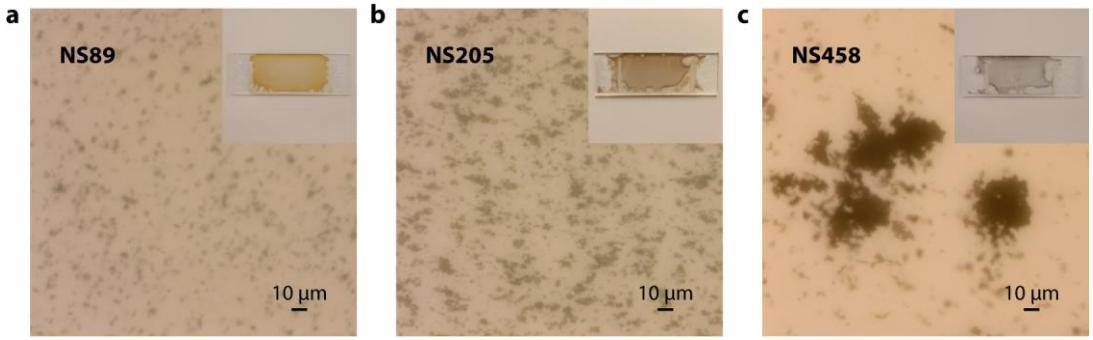

Figure S2. Optical microscopy images of the samples for different sizes of iron oxide nanoparticles encapsulated into a polymer layer. Average diameters were (a) 89 nm, (b) 205 nm, (c) 458 nm. The insets show photographs of the samples.

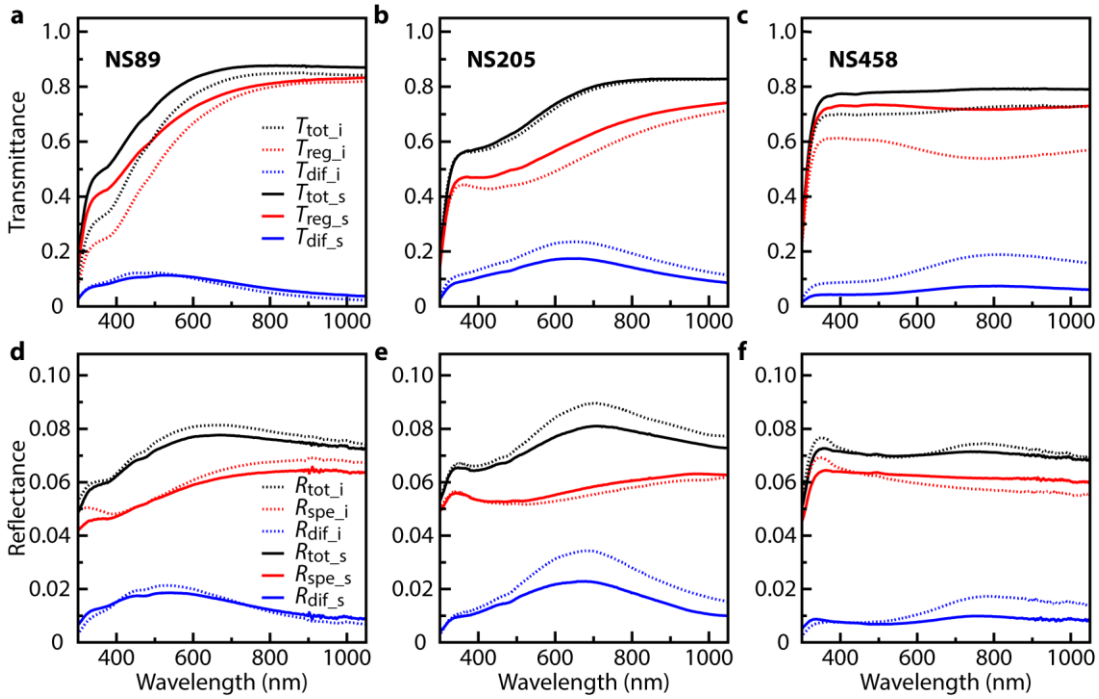

Figure S3. T_{tot}, T_{reg}, T_{dif}, (upper row) R_{tot}, R_{spe}, R_{dif} (lower row) of NS89 (a,d), NS205 (b,e) and NS458 (c,f) samples when in initial state (dotted lines, with subscript *i*) and after 20 days in stable state (solid lines, with subscript *s*). The volume fractions of iron oxide were 0.067% and the thickness of the scattering layers were 72, 76, 76 μm, respectively.

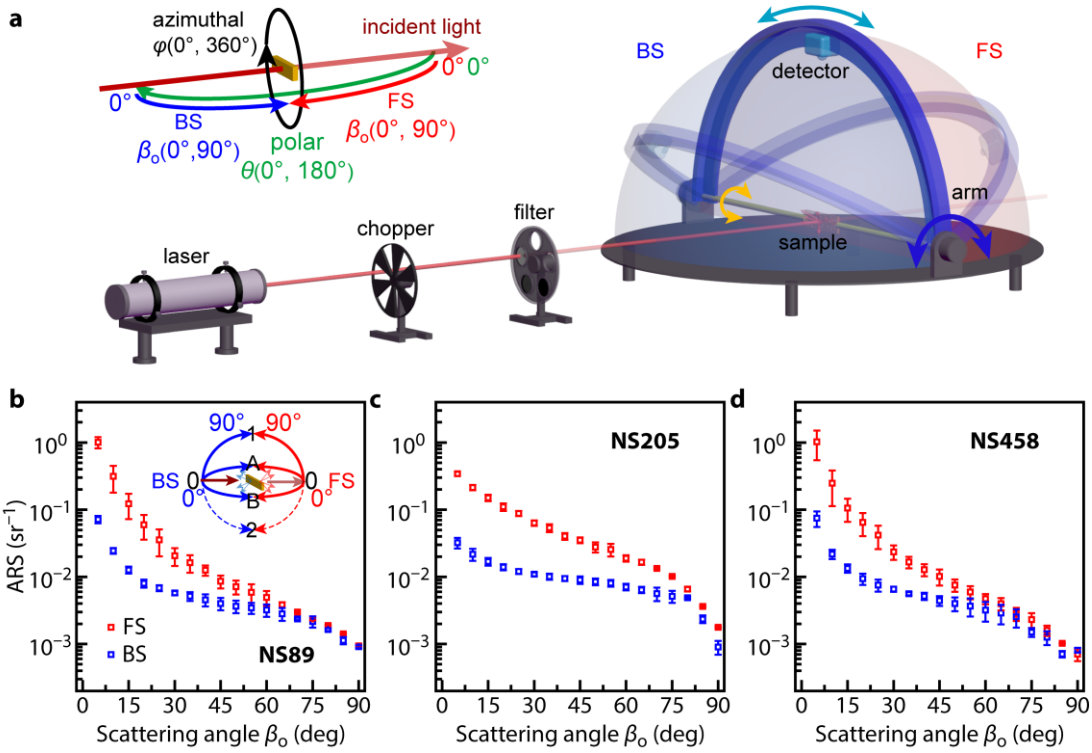

Figure S4. (a) Schematic illustration of out-of-plane goniometer for examination of scattering intensity distribution. The scattered intensity was recorded in a hemisphere, half in transmittance (forward scattering) region, and another half in reflectance (backward scattering) region by the under-illumination method. Inset shows a sketch of the azimuthal angle $\varphi(0°, 360°)$, polar angle $\theta(0°, 180°)$ and scattering angle $\beta_o(0°, 90°)$ in relation to the incident light and the sample. Scattering angle $\beta_o(0°, 90°)$ corresponds to $\theta(0°, 90°)$ in the forward region and $\theta(180°, 90°)$ in the backward region. The average scattering intensities at a wavelength of 633 nm were conducted in four different azimuthal directions [0A, 0B, 01, 02(flip the sample)] in the forward (FS) and backward (BS) hemispheres for (b) NS89, (c) NS205 and (d) NS458 nanocomposite samples as a function of scattering angle. The error bars depict the standard deviations of the four measurements.

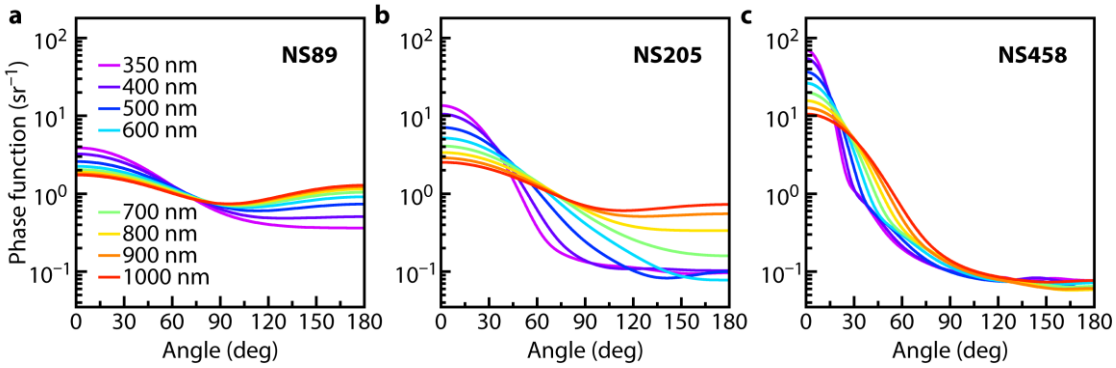

Figure S5. Scattering phase functions computed by Mie theory, considering the size distribution of the nanoparticles, for (a) NS89, (b) NS205 and (c) NS458 Fe_3O_4 nanoparticles at different wavelengths.

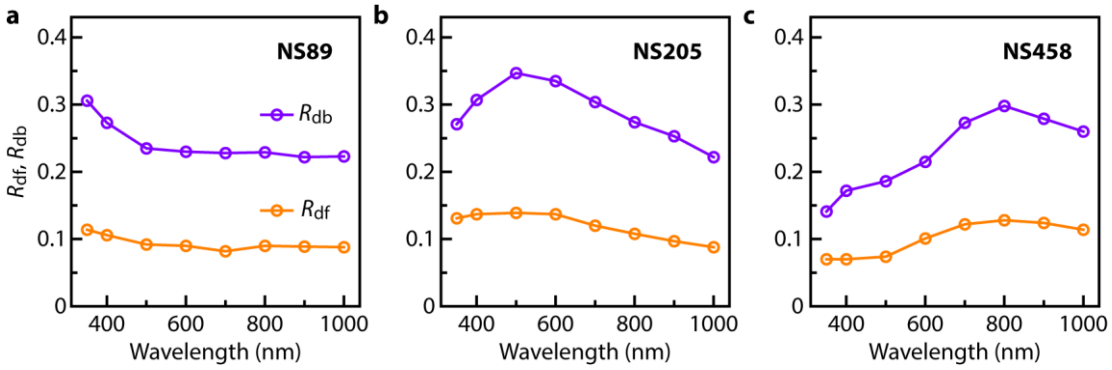

Figure S6. Diffuse reflectances $R_{df,db}$ of light impinging on the back and front interface from the inside of the samples, obtained from calculations using ARS measurements, as described in the main text, for (a) NS89, (b) NS205 and (c) NS458 Fe_3O_4 nanocomposite samples with volume fractions 0.067% and thickness of the scattering layers 72, 76, 76 μm, respectively.

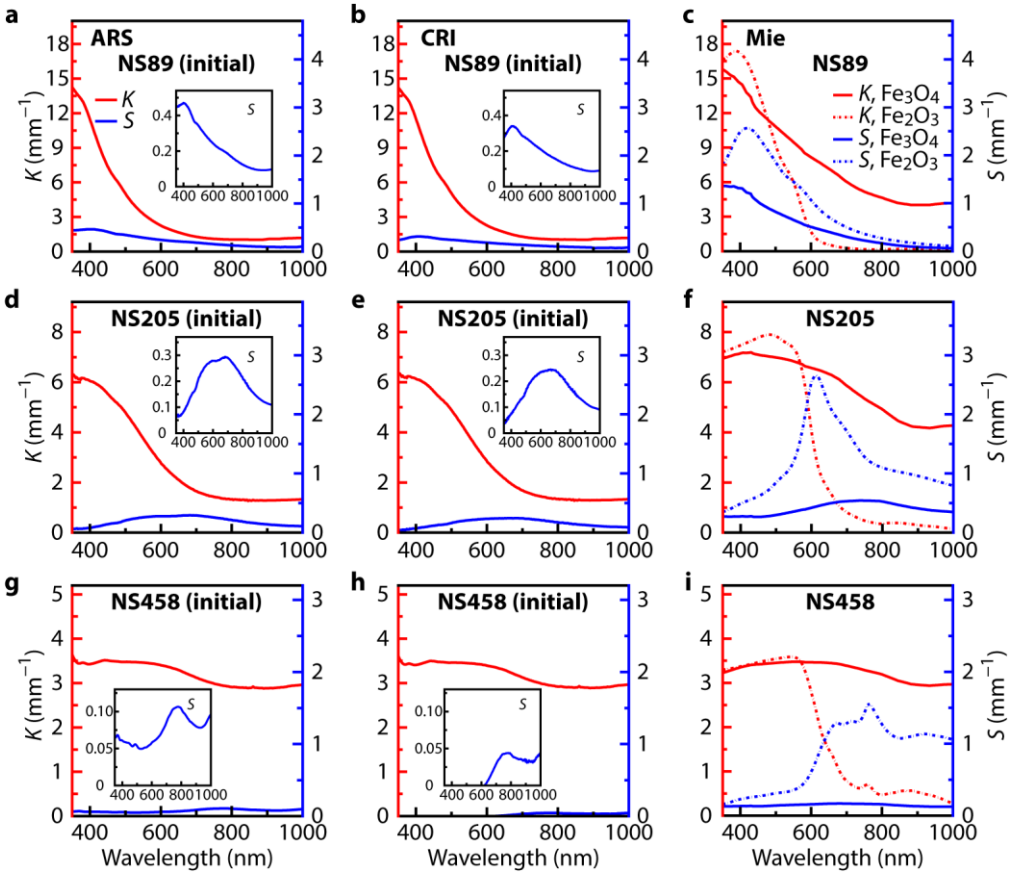

Figure S7. Fitted absorption coefficient *K* (red) and backscattering coefficient *S* (blue) by (a,d,g) ARS and (b,e,h) CRI methods of the NS89, NS205 and NS458 Fe_3O_4 nanocomposite samples in initial state (insets show a zoom-in of the backscattering coefficient *S*). (c,f,i) Simulated *K* (red) and *S* (blue) by Mie theory for Fe_3O_4 (solid) and Fe_2O_3 (dotted) nanocomposites, considering the particle size distributions for the NS89, NS205, and NS458 samples. The volume fractions of iron oxide were 0.067% and the thickness of the scattering layers were 72, 76, 76 μm, respectively.

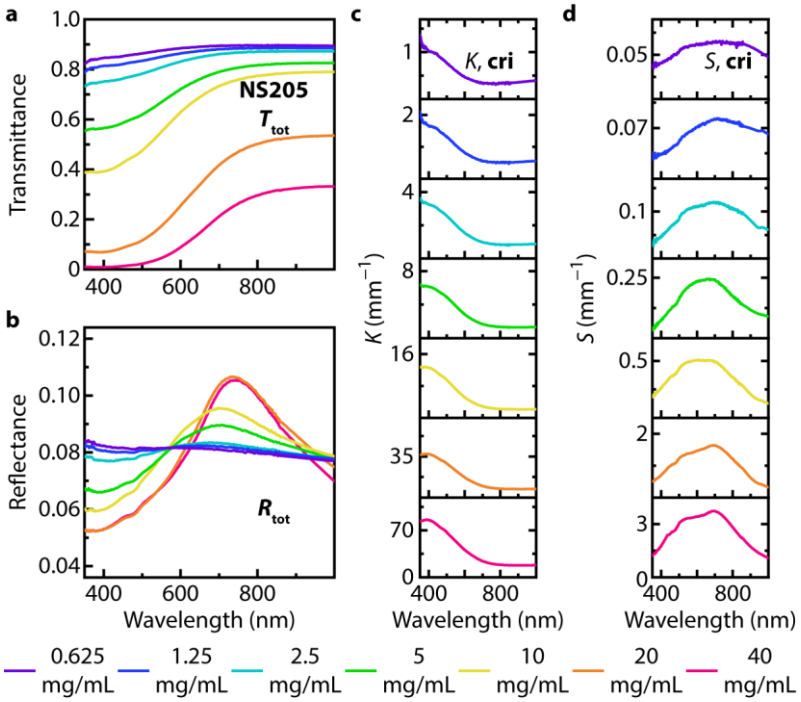

Figure S8. (a) Total transmittance T_{tot}, (b) total reflectance R_{tot}, (c) absorption coefficient K, and (d) backscattering coefficient S for NS205 Fe_3O_4 nanoparticles in water/PVP prepared from water dispersions with particle concentrations of 0.625, 1.25, 2.5, 5, 10, 20 and 40 mg/mL (see legend below figure) in initial state.

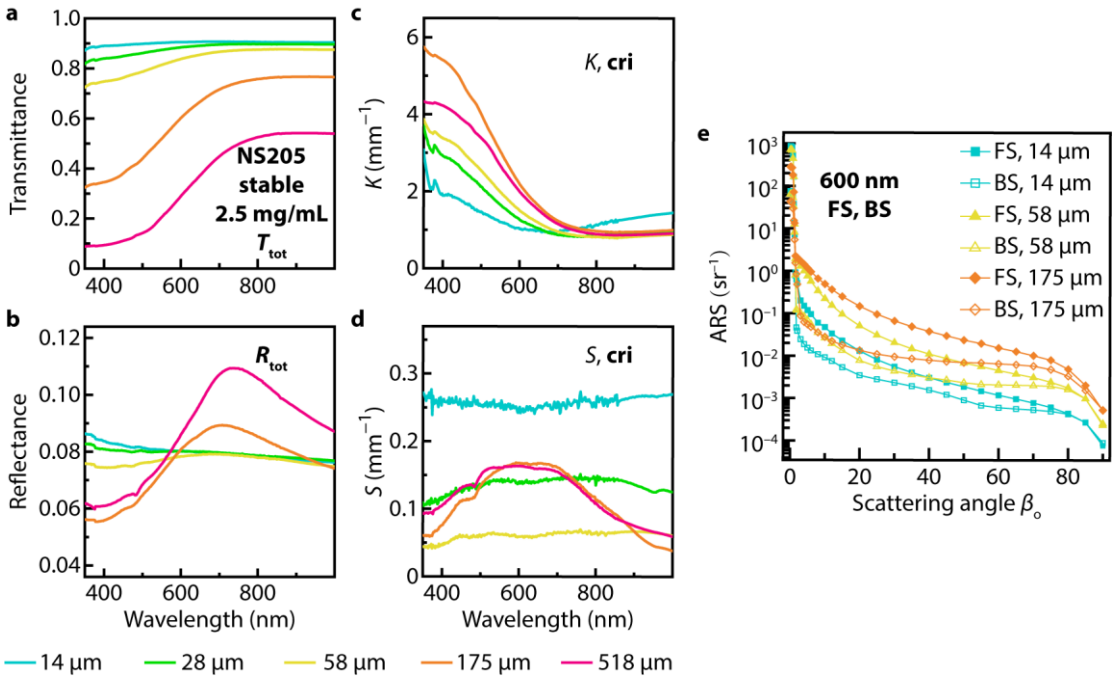

Figure S9. (a) Total transmittance T_{tot}, (b) total reflectance R_{tot}, (c) absorption coefficient K, and (d) backscattering coefficient S of Fe_3O_4 NS205 nanoparticles in water/PVP prepared from a water dispersion with a concentration of 2.5 mg/mL for various thicknesses (see legend below figure) in stable state. (e) Forward and backward scattered intensity as a function of scattering angle for Fe_3O_4 NS205 nanocomposite samples prepared from water dispersion with a concentration of 2.5 mg/mL and different thicknesses.

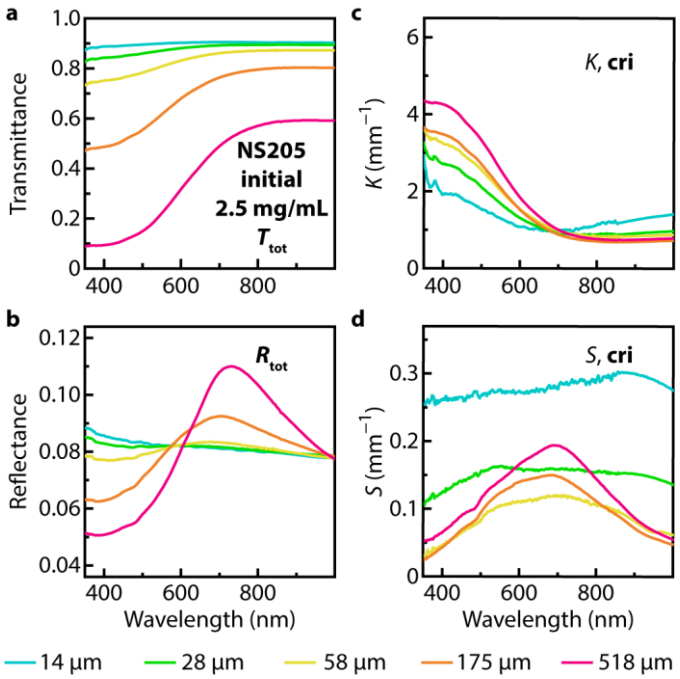

Figure S10. (a) Total transmittance T_{tot}, (b) total reflectance R_{tot}, (c) absorption coefficient K, and (d) backscattering coefficient S of Fe_3O_4 NS205 nanoparticles in water/PVP prepared from a water dispersion with a concentration of 2.5 mg/mL for various thicknesses (see legend below figure) in initial state.

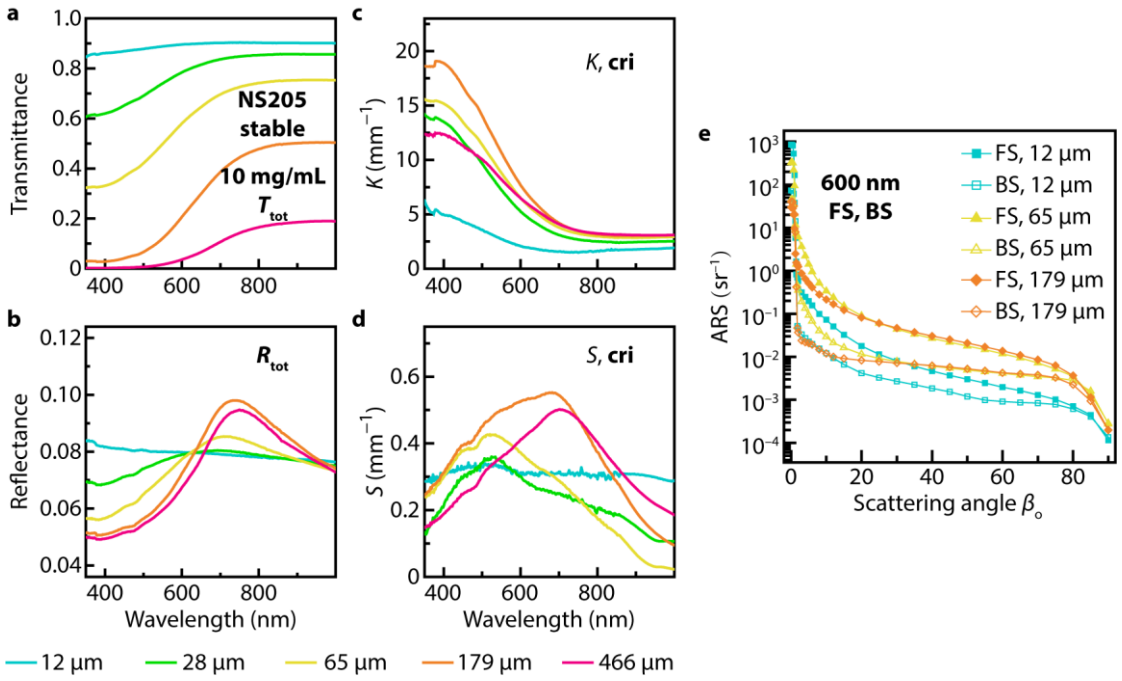

Figure S11. (a) Total transmittance T_{tot}, (b) total reflectance R_{tot}, (c) absorption coefficient K, and (d) backscattering coefficient S of Fe_3O_4 NS205 nanoparticles in water/PVP prepared from a water dispersion with a concentration of 10 mg/mL and various thicknesses (see legend below figure) in stable state. (e) Forward and backward scattered intensity as a function of scattering angle for Fe_3O_4 NS205 nanoparticles in water/PVP prepared from a water dispersion with a concentration of 10 mg/mL and different thicknesses.

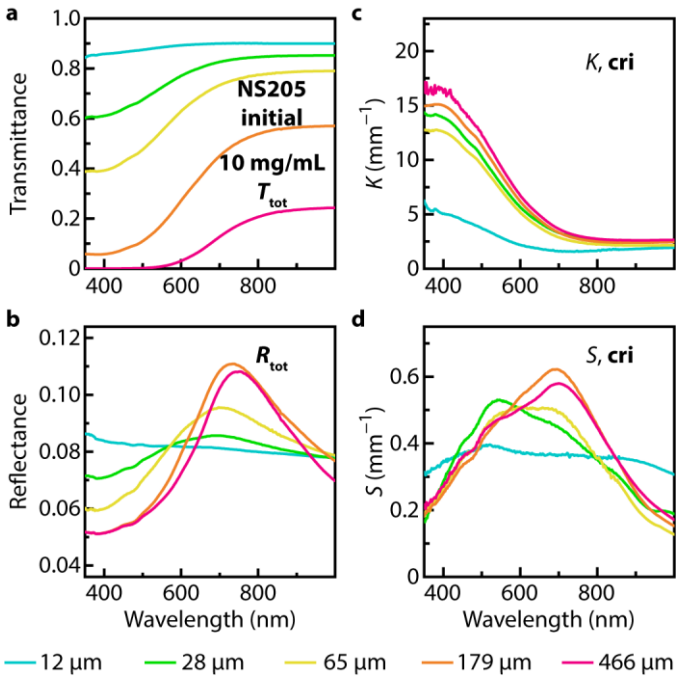

Figure S12. (a) Total transmittance T_{tot}, (b) total reflectance R_{tot}, (c) absorption coefficient K, and (d) backscattering coefficient S of Fe_3O_4 NS205 nanoparticles in water/PVP prepared from a water dispersion with a concentration of 10 mg/mL for various thicknesses (see legend below figure) in initial state.

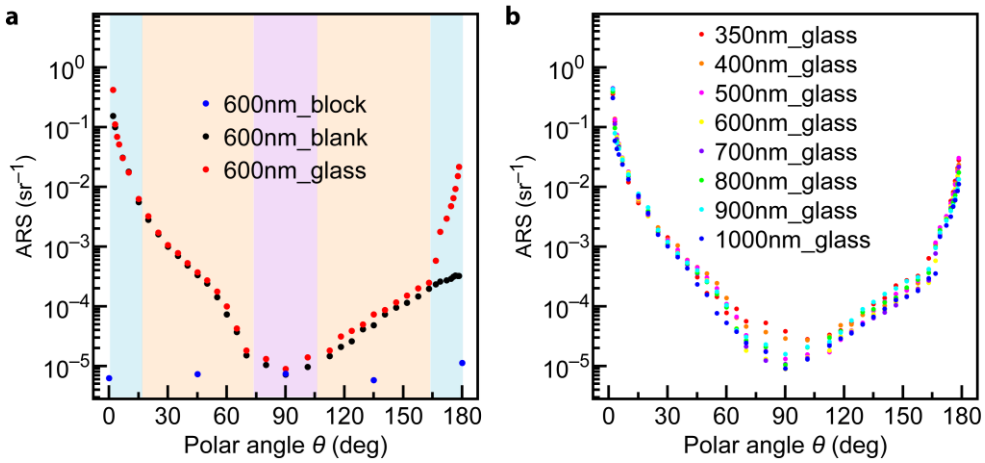

Figure S13. ARS scattering intensity measured by the in-plane scatterometer, (a) at a wavelength of 600 nm, with a blocked light beam ("block"), with light but without any sample ("blank") and using a glass slide at the sample position ("glass") as a function of polar angle from 2° to 178°. (b) Comparison of ARS measurements on the glass slide, as a function of polar angle (from 2° to 178°), conducted at different wavelengths.

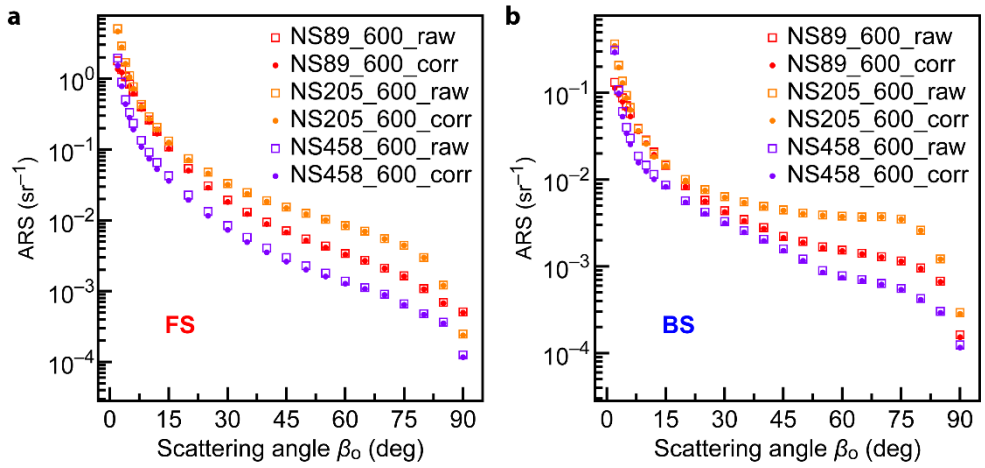

Figure S14. ARS scattering intensity at a wavelength of 600 nm as a function of scattering angle in (a) the forward and (b) the backward direction for Fe_3O_4 nanoparticle samples NS89, NS205 and NS458. The raw data are displayed together with values corrected by subtraction of the measured ARS signal from a glass slide (Fig. S13b). The corrections are seen to be very small and this shows that surface scattering from the glass as well as stray light in the apparatus are not significant in relation to our data for the nanoparticle samples.